The Calculation of the Total and Skin Friction Drags of Bodies of Revolution at Zero Incidence

By

A. D. YOUNG, B.A.

COMMUNICATED BY THE DIRECTOR OF SCIENTIFIC RESEARCH, AIR MINISTRY

Reports and Memoranda No. 1874

27th April, 1939*

SUMMARY. By means of the principles and assumptions used to calculate the profile drag of aerofoils a method is developed for calculating the total and skin friction drags of bodies of revolution at zero incidence. The method is applied to three bodies of different fineness ratio for three Reynolds numbers and three transition points. From the results curves are drawn showing the variation of total drag for a range of fineness ratio (∞ to 3 : 1), Reynolds number (10^6 to 10^8) and transition point position (0 to $0{\cdot}5l$). Comparison with experimental results shows satisfactory agreement.

Interesting deductions are :

(*a*) $\dfrac{\text{form drag}}{\text{total drag}} = 0{\cdot}4\ d/l$, approx.

(*b*) Given the volume and transition point position the fineness ratio for which the drag is least is about 5 : 1.

(*c*) Given the frontal area and transition point position the fineness ratio for which the drag is least is about 3 : 1.

LIST OF SYMBOLS

x	distance along surface from stagnation point or distance along centre line of wake,
y	distance measured normal to surface or normal to centre line of wake,
r	radius of cross section of body,
ξ	distance measured parallel to axis of body from stagnation point,
α	angle between tangent to generator and axis of body,
l	length of body,
d	maximum diameter of body,
A	surface area of body,
$f(d/l)$	A/l^2,
U_0	velocity of undisturbed stream,
U	velocity at edge of boundary layer or wake,
u	velocity in boundary layer parallel to surface or in wake parallel to centre line,
δ	boundary layer thickness or radius of cross section of wake,
Λ	displacement area of boundary layer $= 2\pi\int_0^{\delta}\left(1-\frac{u}{U}\right)(r+y\cos\alpha)\,dy$, displacement area of wake $= 2\pi\int_0^{\delta}\left(1-\frac{u}{U}\right)y.dy$,
δ^*	displacement thickness of boundary layer $= \Lambda/2\pi r$,
$\varkappa$	momentum area of boundary layer $= 2\pi\int_0^{\delta}\frac{u}{U}\left(1-\frac{u}{U}\right)(r+y\cos\alpha)\,dy$, momentum area of wake $= 2\pi\int_0^{\delta}\frac{u}{U}\left(1-\frac{u}{U}\right)y.dy$,

* R.A.E. Report, April, 1939.

LIST OF SYMBOLS—*contd.*

θ	momentum thickness of boundary layer $= \varkappa/2\pi r$
H	$\Lambda/\varkappa$,
p	pressure in boundary layer or wake,
p_δ	pressure at outer edge of boundary layer or wake,
D	drag of body,
C_A	total drag coefficient $= D/\frac{1}{2}\varrho U_0^2 A$,
τ_0	intensity of skin friction,
c_f	local skin friction coefficient $= 2\tau_0/\varrho U_0^2$,
C_f	skin friction drag coefficient $= \int_0^l \frac{1}{c_f} c_f . 2\pi r . d\xi$,
ν	kinematic viscosity,
z	δ^2/ν,
λ	$U'z$,
ζ	$(\varrho U_0^2/\tau_0)_{\frac{1}{2}}$,

dashes denote differentiation with respect to x, suffix 1 denotes that quantities have their values at the tail.

---

1. *Introduction.*—By a modification of the method used to calculate the profile drag of aerofoils[1] a method has been developed for calculating the drag of smooth bodies of revolution. This method has been applied to three bodies at zero incidence, the calculations covering a wide range of fineness ratio, Reynolds number and transition position. It is hoped that the results of these calculations will be of particular value to those engaged in performance estimation and in research relating to the cleanness efficiency of aeroplanes.

2. *Preliminary discussion.*—The flow in the boundary layer of a streamline body has the same characteristics as the flow in the boundary layer of an aerofoil[1]. Consider a streamline body at zero incidence as shown in Fig. 1. Starting from the stagnation point A there is a boundary layer present over the surface of the body. The flow in the boundary layer is laminar for some distance to T, say, then follows a transition region, after which the flow in the boundary layer becomes fully turbulent. From the tail the boundary layer continues downstream as the wake.

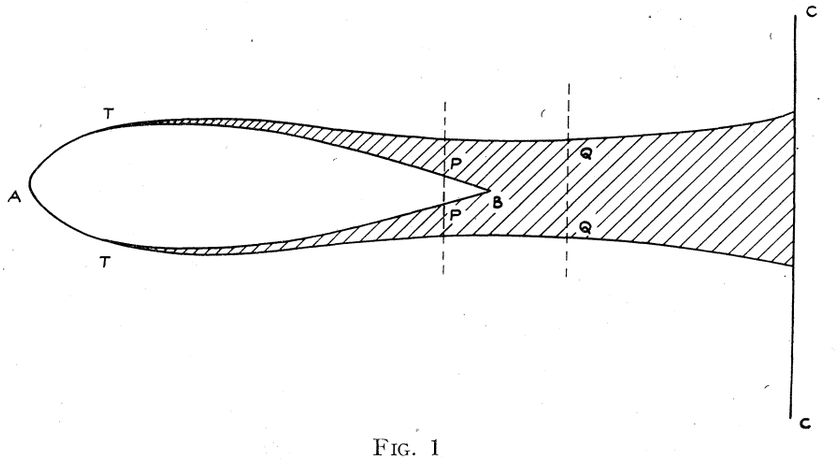

FIG. 1

Consider the section of the wake CC sufficiently far downstream for the static pressure to be equal to that of the free stream. Then from momentum considerations it is easy to see that the drag of the body is given by

$$D = 2\pi\varrho \int_0^\infty u\,(U_0 - u)y.dy, \quad .. \quad .. \quad .. \quad .. \quad (1)$$

where U_0 is the velocity of the free stream, u is the velocity in the wake parallel to the main stream, ϱ is the density of the air assumed incompressible and y is measured normal to the centre line of the wake in the measurement plane. Since u is equal to U_0 outside the wake the integrand vanishes there. The drag coefficient of the body is defined by

$$C_A = D/\tfrac{1}{2}\varrho U_0^2 A, \qquad (2)$$

where A is the surface area of the body. The momentum area of the wake far downstream is defined by

$$\varkappa_0 = 2\pi \int_0^\infty \frac{u}{U_0}\left(1 - \frac{u}{U_0}\right) y.dy. \qquad (3)$$

From (1) and (2) it follows that

$$C_A = \frac{2}{A}.2\pi \int_0^\infty \frac{u}{U_0}\left(1 - \frac{u}{U_0}\right) y.dy = \frac{2\varkappa_0}{A}. \qquad (4)$$

This relation shows that the drag coefficient of the body can be obtained if the momentum area of the wake far downstream can be calculated.

If τ_0 is the skin friction at a point of the surface of the body and r the local radius of cross section the skin friction drag coefficient of the body C_f is given by

$$C_f = \frac{2}{A}\int_0^l \frac{\tau_0}{\varrho U_0^2} \cdot 2\pi r.d\xi, \qquad (5)$$

where ξ is measured parallel to the axis of the body from the nose and l is the length of the body.

The analysis proceeds on similar lines to that described in R. & M. 1838[1]. With a given pressure distribution on a streamline body the development of the boundary layer is followed from the forward stagnation point. The boundary layer is assumed to be laminar for a certain distance. Transition is assumed to occur suddenly and the development of the fully turbulent boundary layer is then followed to the tail; the distributions of the skin friction and of the boundary layer momentum area over the surface of the body are thus obtained. The wake is investigated on the assumption that its momentum area at the tail is equal to that of the boundary layer there. The value of the wake momentum area far downstream is derived from the momentum equation of the wake, the profile drag coefficient is then determined from equation (4). The calculations thus give both the total and skin friction drags, the difference is presumably the form drag.

3. *Details of method*—3.1. *Laminar layer.*—Tomotika's method is used to determine the skin friction and boundary layer thickness of the laminar layer. This method is an extension to three dimensions of Pohlhausen's method[3]. It requires the solution of the equation

$$\frac{dz}{dx} = \frac{f(\lambda)}{U} - \left(\frac{r'}{r}\cdot\frac{U}{U'}\right)\frac{f^*(\lambda)}{U} + z^2\, U''\, g(\lambda) \qquad (6)$$

where $z = \delta^2/\nu$, $\lambda = U'z$,

x is the distance measured along a generator of the surface from the stagnation point,

δ is the boundary layer thickness,

U is the velocity at the edge of the boundary layer,

ν is the kinematic viscosity of the fluid,

$f(\lambda)$, $f^*(\lambda)$, and $g(\lambda)$ are functions which are tabulated in Reference 2, and dashes denote differentiation with respect to x.

At the stagnation point $x = 0$, $\lambda = 4{\cdot}716$. Equation (6) was solved by a step-by-step method up to the assumed transition points.

As in two dimensions the skin friction at the surface is given by

$$\tau_0 = \frac{\mu(\lambda + 12)\,U}{6\delta},$$

and the local skin friction coefficient is given by

$$c_f = \frac{2\tau_0}{\varrho U_0^2} = \frac{(\lambda + 12)\nu U}{3\delta U^2}.$$

The momentum thickness of the boundary layer is defined by

$$\theta = \int_0^\delta \frac{u}{U}\left(1 - \frac{u}{U}\right)\left(1 + \frac{y}{r}\cos\alpha\right) dy,$$

where u is the velocity in the layer parallel to the surface, y is measured normal to the surface, and α is the angle between the tangent to the generator and the axis of the body. Millikan[4] has shown that the term $y/r.\cos\alpha$ may be neglected for the laminar layer, hence

$$\theta = \int_0^\delta \frac{u}{U}\left(1 - \frac{u}{U}\right) dy.$$

θ is related to δ by

$$\frac{\theta}{\delta} = \frac{5328 - 48\lambda - 5\lambda^2}{45360} \quad . \quad . \quad . \quad . \quad . \quad . \quad (7)$$

The momentum area of the boundary layer is defined by

$$\varkappa = 2\pi \int_0^\delta \frac{u}{U}\left(1 - \frac{u}{U}\right)(r + y\cos\alpha)\, dy$$

$$= 2\pi r.\theta. \quad . \quad . \quad . \quad . \quad . \quad . \quad . \quad (8)$$

Having obtained the distributions of z and therefore δ by means of equation (6), the distributions of θ and $\varkappa$ can be obtained by means of equations (7) and (8).

3.2 *The transition point.*—Strictly speaking the transition to turbulent flow in the boundary layer takes place over a region. For experiments in very turbulent airstreams and at low Reynolds numbers this region may be extensive, but the available evidence suggests that in low-turbulence streams or at moderate and high Reynolds numbers the transition region is small and may be represented by a point. Any discontinuity in the momentum area would require the introduction of an impulse, it follows that the momentum area must be continuous at the transition point.

3.3. *The turbulent layer.*—The momentum equation of the boundary layer is

$$-\frac{\delta}{\delta x}\int_0^\delta 2\pi\varrho(r + y\cos\alpha)\, u^2 dy + U\frac{\delta}{\delta x}\int_0^\delta 2\pi\varrho(r + y\cos\alpha)\, u\, dy - \frac{\delta}{\delta x}\int_0^\delta p\, 2\pi(r + y\cos\alpha)\, dy$$

$$+ p_\delta \frac{\delta}{\delta x}\int_0^\delta 2\pi(r + y\cos\alpha)\, dy = \tau_0\, 2\pi r, \quad . \quad . \quad . \quad . \quad (9)$$

where p is the pressure in the boundary layer, and p_δ is the pressure at the outer edge of the boundary layer. Assuming that p is constant across the boundary layer*, then it follows from Bernouilli's equation which holds outside the boundary layer that

$$\frac{\delta p}{\delta x} = -U\frac{\delta U}{\delta x}.$$

* See Appendix I for discussion of effect of variation of p across the boundary layer.

Equation (9) therefore becomes

$$\frac{\delta}{\delta x}\int_0^\delta 2\pi\varrho(r + y\cos\alpha)\, u\,(U - u)dy + \frac{\delta U}{\delta x}\int_0^\delta 2\pi\varrho(r + y\cos\alpha)\,(U - u)\,dy = \tau_0 \,.\, 2\pi r,$$

or

$$\frac{\delta}{\delta x}(\varrho U^2\varkappa) + \frac{\delta U}{\delta x}\,(\varrho U\Lambda) = \tau_0 \,.\, 2\pi r, \quad .. \quad .. \quad .. \quad .. \quad .. \quad (10)$$

$$\text{where } \Lambda = 2\pi\int_0^\delta (1 - \frac{u}{U})\,(r + y\cos\alpha)\,dy$$

$$= 2\pi r\delta^*, \text{ say.}$$

Writing

$$\frac{\Lambda}{\varkappa} = \frac{\delta^*}{\theta} = H, \text{ equation (10) becomes}$$

$$\frac{\delta\varkappa}{\delta x} + \frac{U'}{U}(H + 2)\varkappa = \frac{\tau_0}{\rho U^2} \,.\, 2\pi r\ldots \quad .. \quad .. \quad .. \quad .. \quad .. \quad (11)$$

It is argued in R. & M. 1838[1] that the relation between τ_0, U and θ that holds for a flat plate would hold with sufficient accuracy between the local values of these quantities on an aerofoil. This is equivalent to neglecting the effect on this relation of the pressure gradients at the surface of the aerofoil. Since the pressure gradients at the surface of bodies of revolution are small the same relation between τ_0, U and θ may be again assumed here. This relation is

$$\frac{U\theta}{\nu} = A\, e^{B\zeta} \quad .. \quad .. \quad .. \quad .. \quad .. \quad .. \quad (12)$$

$$\text{where } \zeta = \left(\frac{\varrho U^2}{\tau_0}\right)^{\frac{1}{2}},$$

$$A = 0{\cdot}2454, \text{ and } B = 0{\cdot}3914.$$

From (12) it follows that

$$\frac{U\varkappa}{\nu} = A \,.\, 2\pi r e^{B\zeta}, \quad .. \quad .. \quad .. \quad .. \quad .. \quad (13)$$

$$\text{therefore } \frac{\tau_0}{\varrho U^2} = B^2/\log^2 e\left[\frac{U\varkappa}{A \,.\, 2\pi r\nu}\right].$$

Hence (11) becomes

$$\frac{d\varkappa}{dx} + \frac{U'}{U}(H + 2)\varkappa = 2\pi r B^2/\log^2 e\left[\frac{U\varkappa}{A \,.\, 2\pi r\nu}\right]\ldots \quad .. \quad .. \quad .. \quad (14)$$

As in two dimensions we assume H is constant over the body and equal to 1·4 (cf. Reference 5).

Given U and r as functions of x and the initial value of $\varkappa$ at the transition point equation (14) can be solved for $\varkappa$ by a step-by-step process. The skin friction distribution over the body is given directly by the term on the right hand side of equation (14).

3.4. *The wake.*—In the wake the value of H falls steadily from its value at the trailing edge to the value unity far downstream. The skin friction term in the momentum equation of the wake is zero, hence that equation is

$$\frac{d\varkappa}{dx} + \frac{U'}{U}(H + 2)\varkappa = 0, \quad .. \quad .. \quad .. \quad .. \quad .. \quad .. \quad .. \quad (15)$$

where x is now measured downstream from the tail along the axis of symmetry.

It will be seen that this equation has the same form as equation (12) of R. & M. 1838[1], and can therefore be solved in the same manner. Thus rewriting it, we have

$$\frac{1}{\chi}\cdot\frac{d\chi}{dx} = -(H+2)\frac{d}{dx}(\log_e\frac{U}{U_0}),$$

where U_0 is the velocity of the stream at infinity. Integrating from the tail to infinity we obtain

$$\left[\log \chi\right]_\infty^T = -\left[(H+2)\log_e\frac{U}{U_0}\right]_\infty^T + \int_\infty^T \log_e\frac{U}{U_0}\cdot\frac{dH}{dx}\cdot dx,$$

$$\text{or } \chi_0 = \chi_1\left(\frac{U_1}{U_0}\right)^{H_1+2}\exp\left[\int_1^{H_1}\log_e\frac{U_0}{U}\cdot dH\right], \quad \ldots \quad (16)$$

where the suffix 1 denotes quantities measured at the tail and suffix o denotes quantities measured at infinity downstream. Since $\frac{U_0}{U}$ and H both decrease continuously from their values at the trailing edge to the value unity at infinity, it follows that

$$0 < \int_1^{H_1}\log_e\frac{U_0}{U}\,dH < (H_1-1)\log\frac{U_0}{U_1}.$$

But in practice the ratio U_0/U is, even for bodies of small fineness ratio, only slightly greater than unity. For example, for the body of fineness ratio 3·25 : 1 considered later in this report (*see* Fig. 2)

$$\frac{U_0}{U} = 1\cdot205.$$

Putting $H_1 = 1\cdot4$, it follows that for this body

$$0 < \int_1^{H_1}\log\frac{U_0}{U}\,dH < 0\cdot075,$$

$$\text{or } 1 < \exp.\left[\int_1^{H_1}\log\frac{U_0}{U}\,dH\right] < 1\cdot075,$$

The range of possible values of $\exp.\left[\int_1^{H_1}\log\frac{U_0}{U}\,dH\right]$ is therefore small and hence a rough approximation to its value is justified. It was assumed in R. & M. 1838[1] that for the flow in the wake of an aerofoil the relation between $\log U_0/U$ and $(H-1)$ was a linear one, there being some experimental evidence to support this assumption. In view of the above, it is quite safe to make the same assumption for the flow in the wake of a streamline body, hence

$$\int_1^{H_1}\log\frac{U_0}{U}\cdot dH = \frac{H_1-1}{2}\log_e\frac{U_0}{U_1}$$

$$\text{or } \exp.\left[\int_1^{H_1}\log\frac{U_0}{U}\,dH\right] = \left(\frac{U_0}{U_1}\right)^{\frac{H_1-1}{2}}. \quad \ldots \quad (17)$$

It follows from (16) that

$$\chi_0 = \chi_1\left(\frac{U_1}{U_0}\right)^{\frac{H_1+5}{2}}. \quad \ldots \quad (18)$$

Putting $H_1 = 1{\cdot}4$, we have

$$\varkappa_0 = \varkappa_1 \left(\frac{U_1}{U_0}\right)^{3{\cdot}2}.$$

Hence, from (4)

$$C_A = \frac{2\varkappa_0}{A} = \frac{2\varkappa_1}{A}\left(\frac{U_1}{U_0}\right)^{3{\cdot}2} \quad \ldots \quad \ldots \quad \ldots \quad \ldots \quad \ldots \quad (19)$$

Thus, having determined the value of $\varkappa$ at the tail C_A can be calculated.

4. *Details of the calculations*—4.1. *Cases considered.*—It was desired to apply the method to a sufficient number of cases to enable interpolations to be made covering a wide range of fineness ratio, Reynolds number and transition point position. The method was therefore applied to three bodies at zero incidence of fineness ratio $9{\cdot}70 : 1^6$, $5{\cdot}9 : 1^7$, and $3{\cdot}25 : 1^8$* for which measured pressure distributions were available. The velocity distributions determined by Bernouilli's equation are shown with the three bodies in Fig. 2 (curves A, B and C). The calculations were made for Reynolds numbers ($U_0 l/\nu$) of 10^6, 10^7, and 10^8 and for transition positions of about 0, $0{\cdot}3l$, and $0{\cdot}6l$ from the nose.

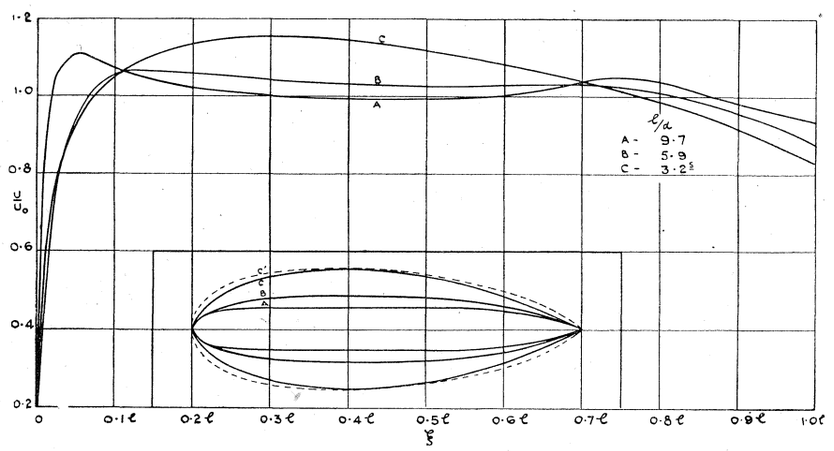

FIG. 2.—Velocity distributions for bodies of revolution of fineness ratio 9·7 : 1, 5·9 : 1, and $3{\cdot}2^5$: 1

It is shown in Appendix II that if the assumptions upon which this method is based remain valid, the drag coefficient of a body of revolution of large fineness ratio tends to the frictional drag coefficient of a flat plate at the same Reynolds number and with the same transition point position. The validity of the assumptions is discussed and it is concluded that it is improbable that they will lead to appreciable errors for the fineness ratios likely to be considered in practice. Since the case of the flat plate has been worked out in detail an additional set of results corresponding to the limiting case of infinite fineness ratio was immediately available.

4.2. *Results of the calculations.*—The numerical results are given in Table 1. Fig. 3, 4 and 5 show the total drag results plotted against fineness ratio, each figure corresponding to a definite value of the Reynolds number. The results have been cross plotted for simplicity in use and are given again in Fig. 6a–6f in which the drag coefficient is plotted against Reynolds number for various fineness ratios, each figure corresponding to a given transition point position measured parallel to the axis from the nose.

* The body considered in Reference 8 actually had a fineness ratio of 3 : 1 but its tail was blunt. By making the tail pointed in agreement with the other bodies chosen the fineness ratio was increased to $3{\cdot}2^5 : 1$. It was assumed that this modification would not affect the pressure distribution.

TABLE 1

Fineness ratio	Distance of T.P. from nose	$R = 10^6$		$R = 10^7$		$R = 10^8$	
		C_A	C_f	C_A	C_f	C_A	C_f
∞	0	0·00461	0·00461	0·00300^5	0·00300^5	0·00214	0·00214
∞	0·2l	0·00411	0·00411	0·00259	0·00259	0·00179	0·00179
∞	0·4l	0·00351^5	0·00351^5	0·00211^5	0·00211^5	0·00142	0·00142
∞	0·6l	0·00286	0·00286	0·00160	0·00160	0·00103	0·00103
9·7 : 1	0·06l	0·00480	0·00461^5	0·00313	0·00302	0·00218	0·00211
9·7 : 1	0·26l	0·00412	0·00395^5	0·00255	0·00246	0·00172^5	0·00167
9·7 : 1	0·56l	0·00304	0·00289	0·00170	0·00163^5	0·00108^5	0·00103^5
5·9 : 1	0·046l	0·00508^5	0·00474	0·00334^5	0·00307	0·00234^5	0·00219
5·9 : 1	0·257l	0·00446	0·00423	0·00278^5	0·00260	0·00189	0·00177^5
5·9 : 1	0·534l	0·00315^5	0·00299^5	0·00176	0·00165	0·00114^5	0·00105^5
3·25 : 1	0·044l	0·00619	0·00527	0·00400	0·00344^5	0·00280	0·00243^5
3·25 : 1	0·230l	0·00551	0·00483	0·00348	0·00302	0·00237^5	0·00206^5
3·25 : 1	0·509l	0·00371	0·00323^5	0·00197	0·00174^5	0·00123^5	0·00111

Table of calculated total and skin friction drag values.

An example of the type of skin friction distribution obtained is given in Fig. 7 which shows the quantity $c_f . 2\pi r/l$ plotted against distance along the axis from the nose for the body of fineness ratio 5·9 : 1 at $R = 10^8$ and for three transition point positions. Fig. 8 shows the variation of total drag coefficient C_A and skin friction drag coefficient C_f for this body at $R = 10^8$ with variation of transition point position. The difference between C_A and C_f is presumably due to the form drag which appears as the component of the normal pressures along the direction of flight. The variation of the ratios skin friction drag/total drag and form drag/total drag plotted against

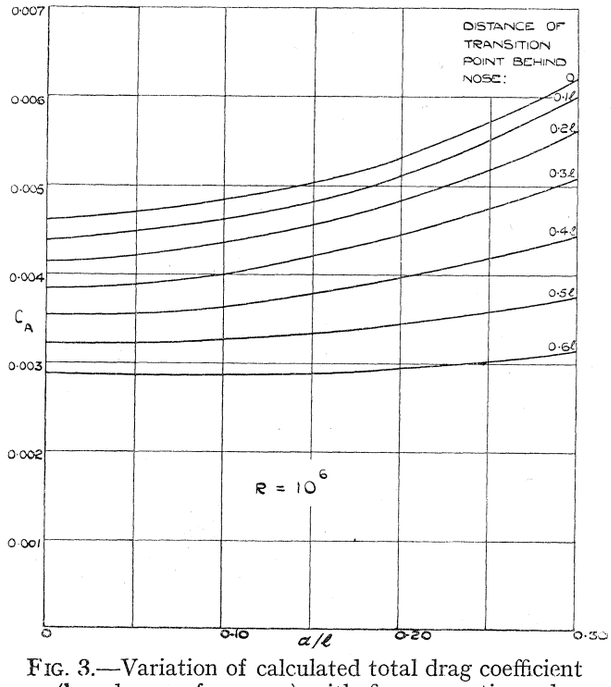

FIG. 3.—Variation of calculated total drag coefficient (based on surface area) with fineness ratio and position of transition point. $R = 10^6$.

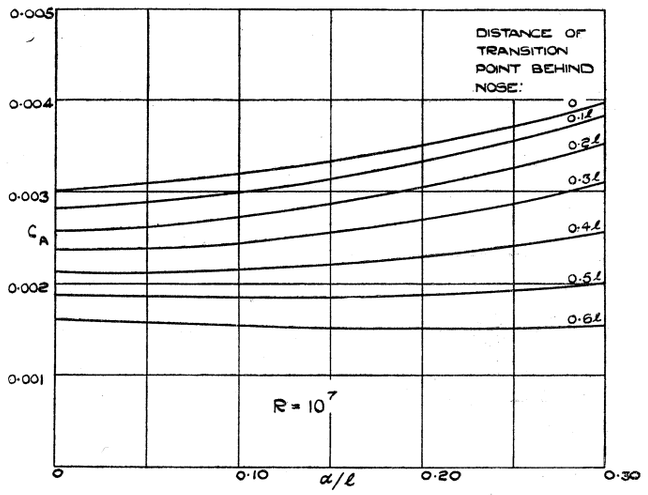

FIG. 4.—Variation of calculated total drag coefficient (based on surface area) with fineness ratio and position of transition point. R=10^7.

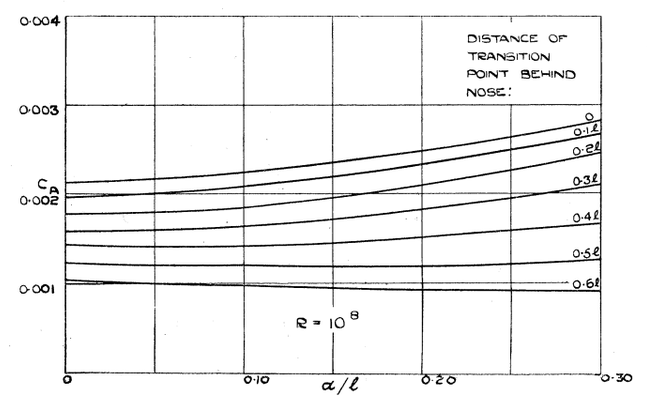

FIG 5.—Variation of calculated total drag coefficient (based on surface area) with fineness ratio and position of transition point. R = 10^8.

fineness ratio for various transition point positions is shown in Fig. 9 ; these ratios were found to be independent of the Reynolds number to the order of accuracy of the calculations. It will be seen that

$$\frac{\text{form drag}}{\text{total drag}} = 0{\cdot}4d/l, \text{ approximately}$$

where d = length of maximum diameter of body. The corresponding formula for aerofoils[1] is

$$\frac{\text{form drag}}{\text{profile drag}} = \text{T/C, approximately.}$$

It follows that the ratio form drag/total drag for a body of revolution is less than half that for an aerofoil of the same thickness and length.

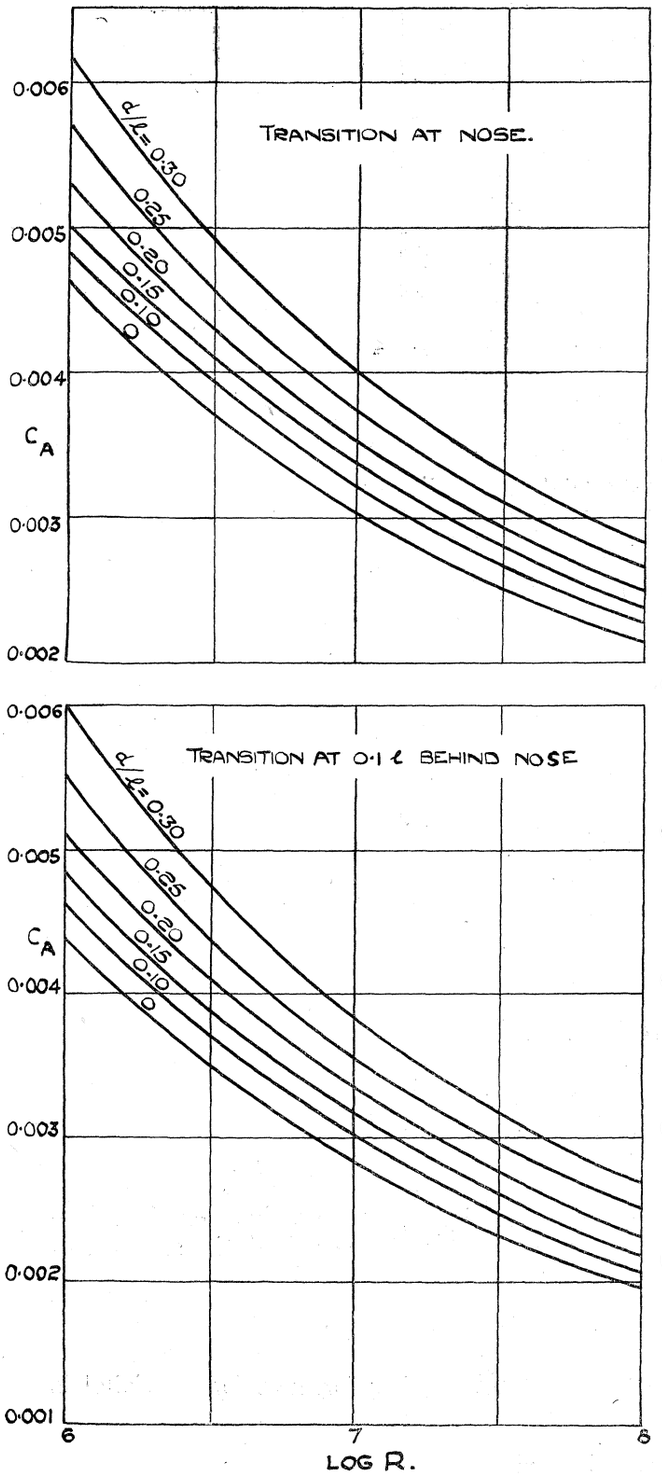

FIG. 6*a* and 6*b*.—Variation of calculated drag coefficient with Reynolds number and fineness ratio. Transition at (*a*) Nose, (*b*) 0·1*l* behind nose.

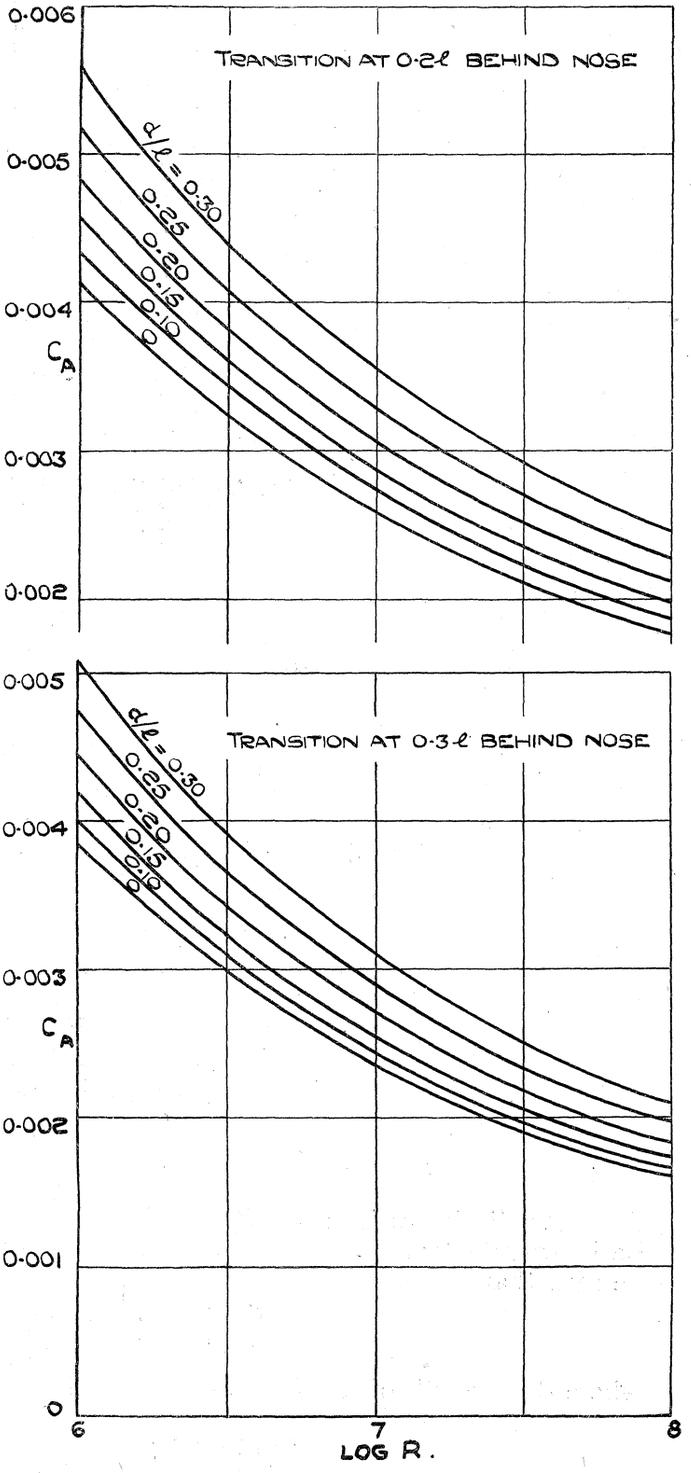

FIG. 6*c* and 6*d*.—Variation of calculated drag coefficient with Reynolds number and fineness ratio. Transition at (*c*) 0·2*l* behind nose, (*d*) 0·3*l* behind nose.

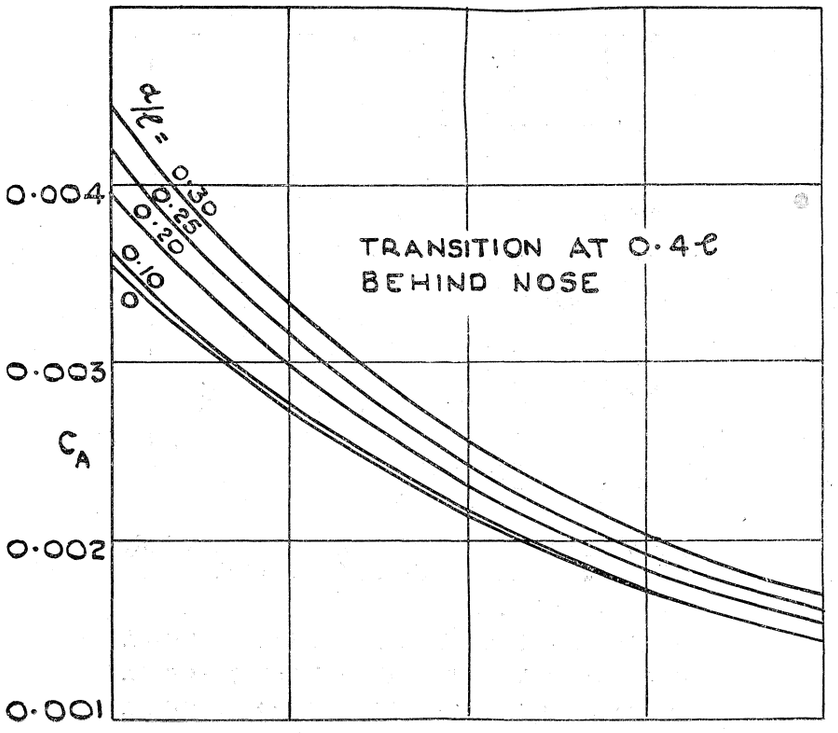

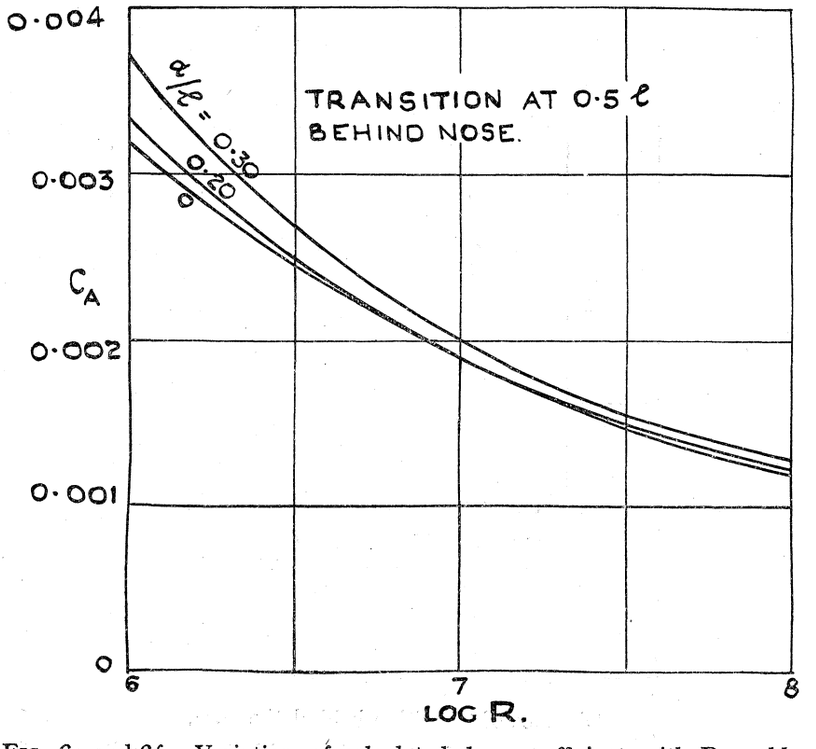

FIG. 6*e* and 6*f*.—Variation of calculated drag coefficient with Reynolds number and fineness ratio. Transition at (*e*) 0·4*l* behind nose, (*f*) 0·5*l* behind nose.

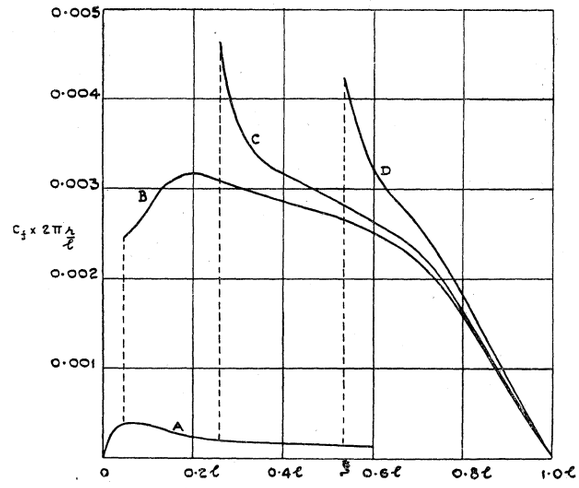

FIG. 7.—Skin friction distribution on streamline body of fineness ratio 5·9 : 1 for R = 10^8.

A—Laminar flow.

B—Turbulent flow. Transition point at $\xi = 0{\cdot}046l$.

C—Turbulent flow. Transition point at $\xi = 0{\cdot}258l$.

D—Turbulent flow. Transition point at $\xi = 0{\cdot}534l$.

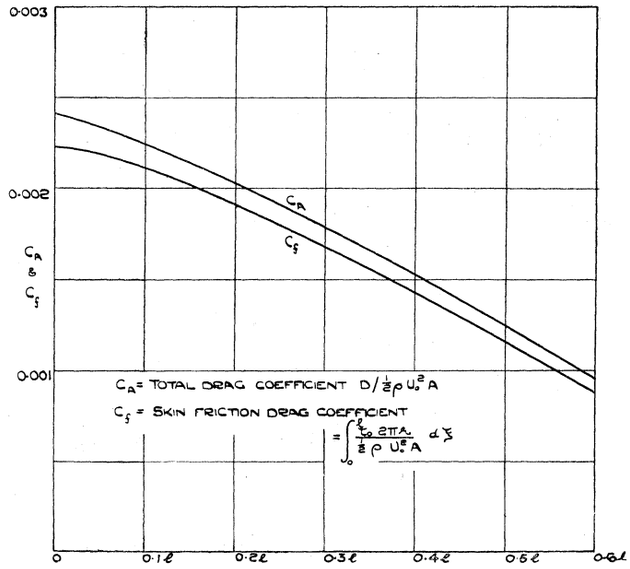

Distance of transition behind the nose.

FIG. 8.—Variation of total and skin friction drag with position of transition for streamline body of fineness ratio 5·9 : 1. R = 10^8.

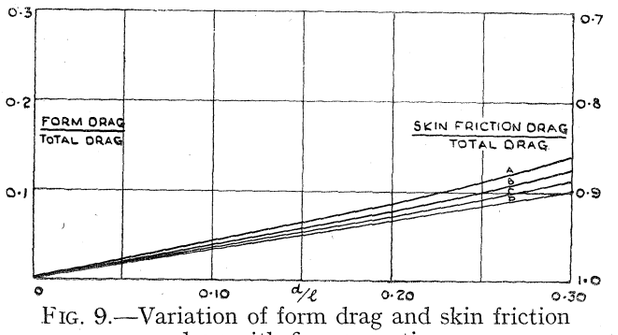

A—Transition at nose
B—Transition at $0 \cdot 2l$
C—Transition at $0 \cdot 4l$
D—Transition at $0 \cdot 6l$.

FIG. 9.—Variation of form drag and skin friction drag with fineness ratio

4.3. *Accuracy of the calculations.*—The remarks made in R. & M. 1888[1] as to the accuracy of the method used to calculate the profile drag of aerofoils apply with little modification here. These, briefly, are as follows.

The arithmetical errors involved in the step-by-step integrations are probably less than 1 per cent. The investigation of the laminar layer by Tomotika's method will be quite accurate for the purpose of these calculations. The assumption of sudden transition to turbulence will introduce errors which will be small if the transition region is short ; it is estimated that a transition region extending over $0 \cdot 05l$ may introduce an error of, at the most, about 3 per cent. The error due to neglecting the effect of the pressure gradient on the relation between U, θ and τ_0 is probably negligible since the pressure gradients on bodies of revolution are generally small. The effect of variations in H from the value assumed near the tail is also negligible.

It is assumed that the transverse pressure gradients across the boundary layer and wake may be neglected although they are appreciable in the region of the tail. This point is discussed in detail in Appendix I where it is concluded that the effect of the transverse pressure gradient near the tail is small and its neglect is therefore justified.

It is to be noted that for bodies of revolution of the same fineness ratio small changes in shape may produce appreciable changes in surface area and therefore in drag. It was necessary to check that the drag coefficient C_A is nevertheless reasonably independent of change in shape. The drag of the body C′ of fineness ratio $3 \cdot 25 : 1$, shown dotted in Fig. 2 was calculated for $R = 10^7$ and for the transition point at $\xi = 0 \cdot 26l$; it was assumed that its velocity distribution was the same as that of the body C of the same fineness ratio. It was found that the drag of C′ was about 5 per cent higher than that of C but its drag coefficient was about 2 per cent low. Had it been possible to allow for the change in velocity distribution with change of shape it is expected that the difference in the drag coefficients would have been even less, since the blunter body would probably have had a slightly higher average velocity over its surface. It can be concluded that small variations in shape have little effect on the drag expressed as a coefficient based on the surface area of the body.

It is to be noted that the method will cease to apply if the boundary layer separates from the body. It follows that the method cannot be used to predict the profile drag of a body for which the boundary layer separates appreciably ahead of the tail. It is known that such separation takes place on bodies of very small fineness ratio, but it is not known how large the fineness ratio must be for separation not to occur. Ower and Hutton[9], however, have found no sign of separation on a body of fineness ratio 3 : 1. Since the smallest fineness ratio considered in these calculations is $3 \cdot 25 : 1$, it is reasonable to suppose that the calculations are quite valid.

4.4. *Comparison with experiment.*—In Table 2 the results of various wind tunnel experiments are compared with the corresponding calculated values. For the results quoted from Miss Lyon's report[5] the transition points were determined from the measured skin friction distributions and the velocity distributions across the boundary layer. In all other cases quoted the transition

points were fixed by wires or strings. It is interesting to note that the agreement between theory and experiment for Model A[5] was not quite so good as the agreement for Model B. This is probably due to the fact that the transition region was longer in the case of Model A and the transition point was therefore more difficult to define. The close agreement between theory and experiment for the body of fineness ratio 3 : 1[1] confirms that boundary layer separation did not occur for this body.

TABLE 2

Reference Numbers	Remarks	$\frac{R}{10^6}$	d/l	Position of T.P. behind nose	C_A measured	C_A calculated
5	Model A (no screen) ..	2·04	0·200	0·60l	0·00220	0·00236
5	Model A (no screen) ..	3·06	0·200	0·52[5]l	0·00220	0·00244
5	Model A (screen) ..	2·09	0·200	0·22l	0·00435	0·00409
5	Model A (screen) ..	3·13[5]	0·200	0·17[5]l	0·00415	0·00388
5	Model B (no screen) ..	2·07[5]	0·200	0·33[5]l	0·00364	0·00361
5	Model B (no screen) ..	3·11	0·200	0·28[5]l	0·00359	0·00351
5	Model B (screen) ..	2·05	0·200	0·15l	0·00440	0·00437
5	Model B (screen) ..	3·07	0·200	0·10l	0·00421	0·00414
10	Model π–Q–12 ..	0·840	0·202	0·10l	0·0053	0·0053
10	N.P.L. short model ..	1·173	0·150	0·10l	0·0045	0·0047
7	1/40th model of "Akron"	11·61	0·170	0·065l	0·0028[5]	0·0030
11	Test done in water ..	1·26	0·182	0	0·0050	0·0050
9 and 12	Body *a*	1·58	0·184	0	0·0045	0·0048
9 and 12	Body B	3·16	0·333	0	0·0050	0·0052
9 and 12	Body *b* ..	1·58	0·333	0	0·0060	0·0062
9 and 12	Body *b*	3·16	0·333	0·04	0·0052	0·0051

Comparison of various measured and calculated drag values.

5. *Some applications.*—Problems which occasionally arise in practice and to which these calculations can be applied are :—

(*a*) Given the volume and forward speed what is the fineness ratio of a streamline body for which its drag will be least.

(*b*) Given the frontal area and forward speed what is the fineness ratio of a streamline body for which its drag will be least.

Consider a representative family of streamline shapes derived from a standard shape such that the radius of a cross section of a member of the family bears a fixed ratio to the radius of the corresponding cross section of the standard shape. If V is the volume and A the surface area of any member of the family, then it is easy to see that

$$\frac{V}{l^3} = K\left(\frac{d}{l}\right)^2, \quad .. \quad .. \quad .. \quad .. \quad .. \quad .. \quad (20)$$

and

$$\frac{A}{l^2} = f\left(\frac{d}{l}\right), \quad .. \quad .. \quad .. \quad .. \quad .. \quad .. \quad (21)$$

where l is the length and d the maximum diameter of the body, K is a constant and $f(d/l)$ is a function of the fineness ratio d/l. Both K and $f(d/l)$ will depend on the standard shape from which the family is derived. Suppose the standard shape is that of the R.101. Then K = 0·465, the function $f(d/l)$ is shown in Fig. 10. As might be expected $f(d/l)$ is very nearly a linear function of d/l. From equation (2)

$$D = C_A \cdot \tfrac{1}{2}\varrho U_0^2 A$$
$$= C_A \cdot \tfrac{1}{2}\varrho U_0^2 \cdot l^2 f\left(\frac{d}{l}\right). \quad .. \quad .. \quad .. \quad .. \quad (22)$$

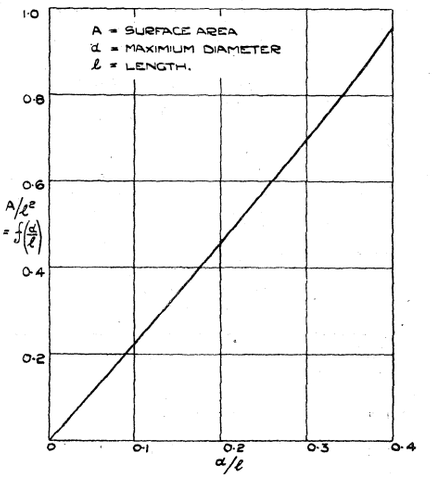

FIG. 10.—Variation of surface area/length^2 with fineness ratio for family of streamline bodies formed from R.101 shape.

(*a*) Consider members of the family of different length and fineness ratio but of equal volume. It follows from equation (20) that

$$d^2 l = \text{const.} \qquad (23)$$

Suppose l_0, and d_0 are the length and maximum diameter of the standard R.101 shape, then

$$(l/l_0) = \left[\left(\frac{d_0}{l_0}\right)\Big/\left(\frac{d}{l}\right)\right]^{2/3}, \qquad (24)$$

$$\text{and } R/R_0 = \left[\left(\frac{d_0}{l_0}\right)\Big/\left(\frac{d}{l}\right)\right]^{2/3}, \qquad (25)$$

$$\text{where } R = \frac{U_0 l}{\nu}, \text{ and } R_0 = \frac{U_0 l_0}{\nu}.$$

If D_0 is the drag of the standard shape, then from (22)

$$D/D_o = \frac{C_A}{C_{A_o}}\left(\frac{l}{l_0}\right)^2 f\left(\frac{d}{l}\right)\Big/ f\left(\frac{d_0}{l_0}\right), \qquad (26)$$

where C_{A0} is the drag coefficient of the standard shape.

Consider the case where the transition point is at the nose for each body and suppose $R_0 = 10^7$. Then, by means of equations (24), (25) and (26) and Fig. 6a and 10 we obtain Table 3. From the first and last columns it will be seen that the drag is least for a body of fineness ratio about 5 : 1. The results are shown again in Fig. 11 where D/D_0 is plotted against d/l. If other values of R_0 and other transition positions are assumed the same result is found, namely, that the optimum fineness ratio is about 5 : 1. It must be noted, however, that the drag is fairly insensitive to quite appreciable variations of the fineness ratio from that value.

TABLE 3

d/l	$A/l^2 = f(d/l)$	l/l_0	R	C_A	D/D_0
0·05	0·114	2·360	$2{\cdot}360 \times 10^7$	0·00271	1·202
0·10	0·229	1·491	$1{\cdot}491 \times 10^7$	0·00301	1·072
0·15	0·342	1·138	$1{\cdot}138 \times 10^7$	0·00329	1·014
0·182	0·413	1·000	$1{\cdot}000 \times 10^7$	0·00347	1·000
0·20	0·456	0·940	$0{\cdot}940 \times 10^7$	0·00356	1·000
0·25	0·570	0·810	$0{\cdot}810 \times 10^7$	0·00386	1·008
0·30	0·692	0·716	$0{\cdot}716 \times 10^7$	0·00422	1·047

Variation of drag of bodies of revolution of equal volume with fineness ratio. Transition at the nose.

(*b*) Consider members of the family of different fineness ratio but having the same frontal area, i.e. all have the same maximum diameter d. If follows that

$$l/l_0 = R/R_0 = \left(\frac{d_0}{l_0}\Big/\frac{d}{l}\right). \qquad .. \quad .. \quad .. \quad .. \quad (27)$$

Assuming as above $R_0 = 10^7$ and the transition point is at the nose in every case, then from equations (26) and (27) and Fig. 6a and 10 we obtain Table 4. The results are also shown in Fig. 12. It will be seen that minimum drag is obtained for a body of fineness ratio about 3 : 1. The same result is found if other values of R_0 and other transition positions are assumed.

TABLE 4

d/l	$A/l^2 = f(d)/l$	l/l_0	R	C_A	D/D_0
0·05	0·114	3·64	$3·64 \times 10^7$	0·00255	2·688
0·10	0·229	1·82	$1·82 \times 10^7$	0·00291	1·544
0·15	0·342	1·214	$1·214 \times 10^7$	0·00326	1·145
0·182	0·413	1·000	$1·00 \times 10^7$	0·00347	1·000
0·20	0·456	0·910	$0·910 \times 10^7$	0·00356	0·942
0·25	0·570	0·728	$0·728 \times 10^7$	0·00394	0·833
0·30	0·692	0·607	$0·607 \times 10^7$	0·00436	0·775
*0·35	0·820	0·520	$0·520 \times 10^7$	0·00495	0·766

* Obtained by extrapolation.

Variation of drag of bodies of revolution of equal frontal area with fineness ratio. Transition at the nose.

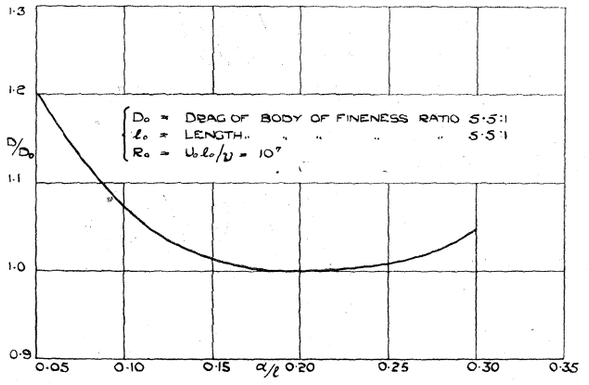

FIG. 11.—Variation of drag of bodies of revolution of equal volume with fineness ratio. Transition at the nose.

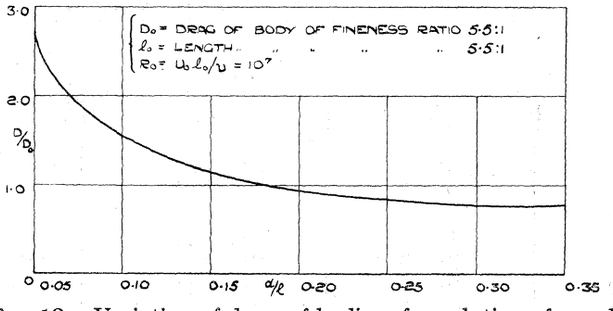

FIG. 12. Variation of drag of bodies of revolution of equal frontal area with fineness ratio. Transition at the nose.

APPENDIX I

6. *Effect of transverse pressure gradients across the boundary layer and wake.*

Equation (9) may be written

$$-\frac{\delta}{\delta x}\int_0^\delta 2\pi\varrho(r+y\cos\alpha)\,u^2\,dy+\mathrm{U}\frac{\delta}{\delta x}\int_0^\delta 2\pi\varrho(r+y\cos\alpha)\,u\,dy$$

$$-\frac{\delta}{\delta x}\int_0^\delta (p-p_\delta)\,2\pi\,(r+y\cos\alpha)\,dy-\frac{\delta p_\delta}{\delta x}\int_0^\delta 2\pi(r+y\cos\alpha)\,dy=\gamma_0\,.\,2\pi r.$$

$$\text{But}\quad \frac{\delta p_\delta}{\delta x}=-\varrho\mathrm{U}\mathrm{U}'.$$

Hence

$$\frac{\delta}{\delta x}\left[\varrho\mathrm{U}^2\varkappa-\int_0^\delta (p-p_\delta)\,2\pi\,(r+y\cos\alpha)\,dy\right]+\mathrm{U}'\,(\varrho\mathrm{U}\Lambda)=\tau_0\,.\,2\pi r. \quad .. \quad (28)$$

Writing

$$\bar{\varkappa}=\varkappa-\int_0^\delta \frac{(p-p_\delta)\,2\pi(r+y\cos\alpha)\,dy}{\varrho\mathrm{U}^2}\,, \quad .. \quad .. \quad (29)$$

$$\text{and}\quad \bar{\mathrm{H}}=\frac{\Lambda}{\chi}. \quad .. \quad .. \quad .. \quad .. \quad .. \quad .. \quad (30)$$

Equation (28) becomes

$$\frac{\delta\bar{\varkappa}}{\delta x}+\frac{\mathrm{U}'}{\mathrm{U}}(\bar{\mathrm{H}}+2)\,\bar{\varkappa}=\frac{\tau_0}{\varrho\mathrm{U}^2}2\pi r. \quad .. \quad .. \quad .. \quad .. \quad .. \quad .. \quad (31)$$

Comparing this equation with equation (11) it will be seen that the two equations are identical except for the substitution of $\bar{\varkappa}$ for $\varkappa$ and $\bar{\mathrm{H}}$ for H. It follows that the process described in this report for determining the drag will be quite accurate if these substitutions are made. It will be seen from (29) that the neglect of the transverse pressure gradients in the region where they are appreciable is equivalent to ignoring the fact that the momentum area in these regions splits up into a kinetic component and a pressure component. However, the transverse pressure gradients are only appreciable in the region of the tail, say from P to Q (Fig. 1). It remains to determine how far this splitting up of the momentum area in that region can affect the final value of the momentum area far downstream.

Let the suffix (calc.) denote quantities calculated on the assumption that the transverse pressure gradients are negligible*, and let a bar denote quantities calculated when allowance is made for those pressure gradients. Then

$$\varkappa_\mathrm{p}\ (\text{calc.})=\bar{\varkappa}_\mathrm{p}.$$

From P onwards these quantities can only differ in so far as they are affected by differences between τ_0 (calc.) and $\bar{\tau}_0$ and between H (calc.) and $\bar{\mathrm{H}}$. But the total effect of the skin friction in the region of the tail is small (cf. equation (14)), hence a small change in the skin friction there can have only a negligible effect. In addition the effect of changing the value of H in the region of the tail to the values that might be expected in practice has already been tested and found to be negligible. It follows that the difference between $\varkappa$ (calc.) and $\bar{\varkappa}$ far downstream cannot be important, and hence the effect of the transverse pressure gradients in the region of the tail on the resulting drag coefficient may be ignored.

* It must be noted that $\varkappa$ (calc.) is not the same as the $\varkappa$ of equation (29) which is only the kinetic component of the momentum area. Hence, if the solution of the wake momentum equation is used to determine the profile drag of a body from measurements made in a plane near its tail, the measured values of $\bar{\varkappa}$ and $\bar{\mathrm{H}}$ must be used.

APPENDIX II

7. *Drag coefficient of body of large fineness ratio.*

For finite l as $l/d \to \infty$, r, r', U′ and U″ all tend to zero. Suppose d is small but finite such that r', U′ and U″ are negligible, then the momentum equation of the boundary layer becomes

$$\frac{d\varkappa}{dx} = \frac{\tau_0}{\varrho U_0^2} 2\pi r.$$

By the definition of θ (equation (8)) this may be written

$$\frac{d\theta}{dx} = \frac{\tau_0}{\varrho U_0^2} = \frac{1}{\zeta^2}. \quad .. \quad .. \quad .. \quad .. \quad .. \quad (32)$$

Since $\lambda = 0$, the velocity distribution in the laminar layer[2] is given by

$$\frac{u}{U_0} = 2\frac{y}{\delta} - 2\frac{y^3}{\delta^3} + \frac{y^4}{\delta^4}. \quad .. \quad .. \quad .. \quad .. \quad .. \quad (33)$$

Hence

$$\theta = \int_0^\delta \frac{u}{U}\left(1 - \frac{u}{U}\right)\left(1 + 2\frac{y}{d}\right)dy$$

$$= 0{\cdot}117\tfrac{5}{2}\delta + 0{\cdot}0794\frac{\delta^2}{d}. \quad .. \quad .. \quad .. \quad .. \quad (34)$$

For the laminar layer

$$\tau_0 = \mu\left(\frac{\delta u}{\delta y}\right)_{y=0} = 2\mu\frac{U_0}{\delta},$$

therefore, from (32) and (34)

$$0{\cdot}117\tfrac{5}{2}\,\delta' + 0{\cdot}1588\,2\frac{\delta}{d}\delta' = \frac{2\nu}{\delta U_0},$$

which integrated gives

$$0{\cdot}117\tfrac{5}{2}\frac{\delta^2}{d^2} + 0{\cdot}106\frac{\delta^3}{d^3} = \frac{4\,x\,l}{R\,d\,d}. \quad .. \quad .. \quad .. \quad .. \quad .. \quad .. \quad (35)$$

The method used in the calculations described in this report for determining the skin friction and momentum thickness distributions in the laminar layer assumes δ/d is negligible compared with 1. Assuming for the moment this is always true, then the second term on the left hand side of equation (35) is negligible compared with the first and therefore

$$0{\cdot}117\tfrac{5}{2}\,\delta^2 = \frac{4xl}{R},$$

or

$$\delta = 5{\cdot}83\sqrt{\frac{lx}{R}}, \quad .. \quad .. \quad .. \quad .. \quad (36)$$

and from (34)

$$\vartheta = 0{\cdot}117\tfrac{5}{2}\,\delta$$

$$= 0{\cdot}684\sqrt{\frac{lx}{R}}. \quad .. \quad .. \quad .. \quad .. \quad .. \quad (37)$$

At the transition point θ is continuous. For the turbulent layer in addition to (32) we have the relation

$$\frac{U_0\theta}{\nu} = 0{\cdot}2454e^{0{\cdot}3914\zeta}. \quad .. \quad .. \quad .. \quad .. \quad .. \quad (38)$$

From (19) we have

$$C_A = \frac{2\chi_1}{A} + \frac{2\chi_1}{2\pi r \,.\, l}$$

$$= \frac{2\theta_1}{l}. \qquad .. \quad .. \quad .. \quad .. \quad .. \quad .. \quad (39)$$

Now consider the case of the flat plate. Parallel to equations (32), (37), (38) and (39) above we have (see References 1 and 13)

$$\frac{d\theta}{dx} = \frac{\tau_0}{\rho U_0^2} = \frac{1}{\zeta^2} \qquad .. \quad .. \quad .. \quad .. \quad .. \quad (32a)$$

For the laminar layer

$$\theta = 0{\cdot}684\sqrt{\frac{lx}{R}} \qquad .. \quad .. \quad .. \quad .. \quad .. \quad (37a)$$

At the transition point θ is continuous. For that turbulent layer

$$\frac{U_0\theta}{\nu} = 0{\cdot}2454e^{0{\cdot}3914\zeta}, \qquad .. \quad .. \quad .. \quad .. \quad .. \quad (38a)$$

and finally the frictional drag coefficient of the plate is given by

$$C_f = \frac{2\theta_1}{l}. \qquad .. \quad .. \quad .. \quad .. \quad .. \quad .. \quad (39a)$$

Hence, if the assumption that δ/d is negligible compared with 1 is valid, the momentum thickness on a body of revolution of large fineness ratio satisfies the same equations and boundary conditions as the momentum thickness on a flat plate. If in the two cases the Reynolds number and transition point position are the same, the momentum thickness at corresponding points must be the same. Therefore, from equations (39) and (39a) the drag coefficient of the body is the same as the frictional drag coefficient of the flat plate.

However, it is apparent from (35) that for large enough values of l/d and x/d and small enough values of R, δ/d will cease to be negligible compared with 1. Assuming that the expression for the velocity distribution given in (33) holds as $d \to 0$, it can be easily seen from (34) and (35) that ultimately

$$\delta \propto (d)^{\frac{1}{3}} \to 0,$$

$$\text{and } \theta \propto \left(\frac{1}{d}\right)^{\frac{1}{3}} \to \infty,$$

and hence, if the boundary layer is laminar for a finite extent,

$$C_A \to \infty.$$

It follows that as the fineness ratio tends to infinity the drag coefficient will begin to rise from the flat plate value at some stage depending on R and the extent of the laminar layer. It was necessary, therefore, to investigate whether at the Reynolds numbers considered in this report this will occur for fineness ratios of practical importance. Using the relations (34) and (35) the drag coefficients of bodies of fineness ratio 100 : 1 and 500 : 1 have been calculated for $R = 10^6$ with the transition points at $x = 0{\cdot}6l$. For the body of fineness ratio 100 : 1 it was found that at the transition point $\delta/d = 0{\cdot}388$, nevertheless, the difference between the resulting value of C_A and the corresponding frictional drag coefficient of the flat plate was inappreciable. For the body of fineness ratio 500 : 1 the difference was only about 4% although $\delta/d = 1{\cdot}377$ at the transition point. There is no available proof that the empirical relation for the turbulent layer given in (38) will continue to hold for very large fineness ratios, but it is believed unlikely that this relation will be in serious error for moderate fineness ratios. It follows that the results and diagrams given in this report will be quite valid for all fineness ratios likely to be considered in practice, although, strictly speaking, they will cease to apply for very large fineness ratios.

LIST OF REFERENCES

No.	*Author*	*Title*
1	H. B. Squire and A. D. Young	The calculation of the profile drag of aerofoils. R. & M.1838 (1937).
2	S. Tomotika	Laminar boundary layer on the surface of a sphere in a uniform stream. R. & M. 1678 (1935).
3	L. Howarth	Steady flow in the boundary layer near the surface of a cylinder in a stream. R. & M. 1632 (1934).
4	C. B. Millikan	The boundary layer and skin friction for a figure of revolution. Trans. Amer. Soc. Mech. Eng. Appl. Mech. Sec. Vol. 54 (1932)
5	H. M. Lyon	A study of the flow in the boundary layer of streamline bodies. R. & M. 1622 (1934).
6	J. R. Pannell, N. R. Campbell and G. N. Pell.	Experiments on model airships. R. & M. 246 (1916).
7	H. B. Freeman	Measurements of flow in the boundary layer of a 1/40th scale model of the U.S. airship " Akron ". N.A.C.A. Report 430 (1932).
8	H. Bateman and F. C. Johansen ..	Pressure and force measurements on airscrew body combinations. R. & M. 1380 (1930).
9	E. Ower and G. T. Hutton	Investigation of the boundary layers and the drag of two streamline bodies. R. & M. 1271 (1929).
10	H. L. Dryden and A. M. Kuethe ..	Effect of turbulence in wind tunnels. N.A.C.A. Report 342 (1930).
11	L. F. G. Simmons and W. C. S. Wigley	The comparison of resistance of bodies in air and water. T.2466 (1927).
12	C. N. H. Lock and F. C. Johansen ..	Drag and pressure distribution experiments on two pairs of streamline bodies. R. & M. 1452 (1932).
13	H. B. Squire	Note on boundary layer flow. R. & M. 1664 (1935).